

The noble gas concentrations of the Martian meteorites

GRV 99027 and paired NWA 7906/NWA 7907

P. C. Stephenson¹, Y. Lin², and I. Leya¹

1. Physical Institute, Space Sciences and Planetology, University of Bern,
Switzerland
2. Key Laboratory of Earth and Planetary Physics, Institute of Geology and
Geophysics, Chinese Academy of Sciences, Beijing, China.

Abstract

Here we present the isotopic concentrations of He, Ne, Ar, Kr, and Xe for the three Martian meteorites Grove Mountains 99027 (GRV 99027), Northwest Africa 7906 (NWA 7906), and Northwest Africa 7907 (NWA 7907). The cosmic ray exposure age for GRV 99027 of 5.7 ± 0.4 Ma (1σ) is consistent with CRE ages for other poikilitic basaltic shergottites and suggests that all were ejected in a single event ~ 5.6 Ma ago. After correcting for an estimated variable sodium concentration, the CRE ages for NWA 7906 and NWA 7907 of 5.4 ± 0.4 , and 4.9 ± 0.4 Ma (1σ), respectively, are in good agreement with the CRE age of ~ 5 Ma favored by Cartwright et al. (2014) for NWA 7034. The data, therefore, support the conclusion that all three basaltic regolith breccias are paired. The ^4He gas retention age for GRV 99027 is not well constrained, but is likely on the order of ~ 54 Ma. The ^{40}Ar gas retention age for NWA 7907 of ~ 1.3 Ga is in accord with Cartwright et al. (2014). For NWA 7906, we were unable to determine a ^{40}Ar gas retention age. The ^4He gas retention ages for NWA 7906 and 7907 are in the range of 200 Ma and are much shorter than the ^{40}Ar gas retention age of NWA 7907, indicating that about 86-88% of the radiogenic ^4He has been lost. The Kr and Xe isotopic concentrations in GRV 99027 are composed almost exclusively of Martian interior gases, while for NWA 7906 and NWA 7907 they indicate gases from the Martian interior, elementally fractionated air, and possibly Martian atmosphere.

INTRODUCTION

The knowledge of cosmic ray exposure histories indicates whether different meteorites arrived on Earth as part of the same fall and are thus paired and/or whether they were ejected from the same parent body during the same event and are hence source crater paired. The exact number of impacts on Mars required to produce the known Martian meteorites is still not well constrained. According to Herzog and Caffee (2014), five ejection events have produced all shergottites found so far, one ejection event produced the nakhlites, one produced ALH84001, one produced NWA 7034 (and paired specimens), and one produced the two chassignites. A more recent study by Irving et al. (2017) reports 14 ejection events for shergottites, with the total number of separate ejection events from Mars being as few as 20.

In this paper, we present the noble gas inventory and cosmic ray exposure (CRE) ages for three Martian meteorites: Grove Mountains 99027 (GRV 99027), Northwest Africa 7906 (NWA 7906), and Northwest Africa 7907 (NWA 7907). The poikilitic basaltic shergottite (formerly termed lherzolitic, Wieler et al. 2016) GRV 99027 has been studied for ^{10}Be and ^{26}Al (Kong et al. 2007) but not for noble gases. NWA 7906 and NWA 7907 are both likely pairs of NWA 7034 (pp. 119-120 of Ruzicka et al. 2015), the unique Martian regolith breccia, but only the latter has been studied for noble gases (Cartwright et al. 2014).

Typically, CRE age studies rely on some type of production rate model (e.g., Eugster and Michel 1995; Leya and Masarik 2009) and assume that all cosmogenic gases have been produced solely from high-energy, deeply penetrating galactic cosmic rays (GCR). However, it seems that Martian meteorites, particularly shergottites, often also contain cosmogenic nuclides produced by solar cosmic rays (SCR) (e.g., Garrison et al. 1995; Wieler et al. 2016). Thus, we must consider any SCR-produced nuclides in our CRE age calculations.

In addition to the noble gases produced by cosmic rays, radiogenic and trapped gases are of importance, as both provide crucial information about the formation and alteration histories of the meteoritic material; thus, they might help confirm or reject whether two meteorites are paired.

EXPERIMENTAL

Bulk samples with masses of ~100 mg consisting of one or several chips were wrapped in commercial aluminum foil and pre-heated in vacuum at ~75°C for ~24 hours to release atmospheric surface contamination. Gases were extracted in six temperature steps at 800°C, 1000°C, 1200°C, 1400°C, 1600°C, and 1740°C. Evolved gases were cleaned by admission to SAES St 707™ getters operating at 280°C. Helium-Ne fractions, Ar fractions, and Kr-Xe fractions were separated from each other using activated charcoals maintained at temperatures between -135°C and -195°C, and ^{40}Ar , ^{84}Kr , and ^{132}Xe were measured in both the Ar and Kr-Xe measurements to account for incomplete separation of the Ar and Kr-Xe fractions. Extraction blanks were determined by analyzing 40 – 60 mg of the same aluminum foil used to wrap the samples and using the same extraction procedure as for the samples. All reported data is corrected for blanks, sensitivity variations, fractionation, and interfering components (where applicable). Reported uncertainties for all values are 1σ , and take into account uncertainties in sample and blank measurements, sensitivity variations, fractionation, and interfering components.

Stepwise blank measurements for GRV 99027 were taken before and after measurement of the sample and the average of the two blanks for each temperature step was used to correct the respective step of the sample measurement. For NWA 7906 and NWA 7907, stepwise blanks were taken before measuring NWA 7906 and between the measurements for NWA 7906 and NWA 7907. The first stepwise blank was measured a few days after loading, pumping, and heating the sample holder and is not as low as the second blank measured after NWA 7906. The first and second blank measurements are generally within a factor of 3 of each other with the exception of Kr, for which the first blank was up to a factor of 10 higher than the second. For NWA 7906 and all isotopes except Kr in NWA 7907, we used the average of the two blanks for each temperature step to correct the respective sample measurement step. For Kr in NWA 7907 we used only the second blank.

The average of the stepwise blank concentrations for the reference isotopes ^3He , ^4He , ^{20}Ne , ^{21}Ne , ^{22}Ne , ^{36}Ar , ^{40}Ar , ^{84}Kr , and ^{132}Xe are given in Table 1 and show typical values for a clean spectrometer. With the exception of ^3He , whose blank is dominated by H_3/HD , blanks are close to atmospheric in isotopic composition.

The blank for ^3He contributes less than 1.2% to the sample gas amounts for almost all measurements. Exceptions are the 1200°C temperature steps for NWA 7906 and NWA 7907, for which the blank contributes more than ~10%, because both samples were already almost degassed (i.e., the measured value does not exceed the blank for the respective temperature step or the uncertainty exceeds the value itself) in the earlier temperature steps. When expressed as a percentage, the blanks for ^4He vary due to large variations in measured ^4He concentrations across different temperature steps and samples. For GRV 99027, the ^4He blank contributes between 3.6% (1200°C) and about 100% (1740°C) to the sample gas amounts. The higher percentage indicates that the sample was essentially degassed for ^4He after the 1200°C temperature step. For NWA 7906 and NWA 7907, the ^4He blank contribution is less than 1% for the 800°C temperature steps and ~14% for the 1200°C temperature steps. Blank contributions for ^{21}Ne are less than 1% for all samples and all temperature steps except the 1600°C (25%) and 1740°C (63%) temperature steps for NWA 7906 and the 1600°C temperature step for NWA 7907 (31%) because the samples were already almost degassed.

Considering only temperature steps up to 1200°C, i.e., temperature steps that are not almost degassed, the ^{36}Ar blanks contribute for all samples less than ~7% to the measured gas amounts. For ^{40}Ar , the blank contributions for all three meteorites are between 1% and 14% if we consider only the temperature steps below (but not including) 1600°C. Interestingly, the high blank contribution of 7% is for the 800°C temperature step of GRV 99027, which has an exceptionally low ^{40}Ar concentration, not only compared to the higher temperature steps of this meteorite but also compared to the ^{40}Ar release pattern for NWA 7906 and NWA 7907.

Technical problems prevented the measurement of some of the Kr and Xe isotopes in GRV 99027 during various temperature steps. For all three samples, ^{84}Kr blanks contribute between 6-12% in the temperature range 800°C-1200°C. Finally, for samples NWA 7906 and NWA 7907, the blank contribution for ^{132}Xe is between 8%-21% for all temperature steps, except for the 1400°C step for NWA 7906, where it was 62%. For GRV 99027, the blank contribution for ^{132}Xe ranges between 2.3% for the 1400°C temperature step and 9% for the 1000°C temperature step.

The ^{20}Ne signals were corrected for interferences from water with mass 20 and $^{40}\text{Ar}^{2+}$; the corrections were always smaller than 8%, with the exception of the 800°C and 1600°C steps of GRV 99027, where it was ~28% and ~18%, respectively. The ^{22}Ne signals were corrected for interferences from CO_2^{2+} ; the corrections never exceeded ~6.4%. Hydrocarbon interferences on Kr isotopes were monitored using mass 77 as a proxy. Since the $^2\text{H}-^1\text{H}$ and the hydrocarbon backgrounds in the spectrometer were the same for the sample and blank measurements, any interfering contributions from these on ^3He and the Kr isotopes, respectively, were corrected by blank subtraction. Mass fractionation and instrument sensitivity were determined by peak height comparisons with signals from calibration gases with known amounts of He, Ne, Ar, Kr, and Xe. The calibration gases were of atmospheric isotopic composition, with the exception of ^3He , which was artificially enriched.

We calculated new cosmogenic production rates and CRE ages using two versions of the Leya and Masarik (2009) model. For GRV 99027, we used two extended versions (one for noble gases and one for ^{10}Be) tailored specifically for small ($\leq 7\text{cm}$) shergottites. However, this model is valid only for small shergottites and cannot be used on larger meteorites like NWA 7906 and NWA 7907. Both extended models are available upon request from one of the co-authors (IL). Production rates and CRE ages for NWA 7906 and NWA 7907 were calculated using the production rate model of Leya and Masarik (2009) for ordinary chondrites, which was also used by Cartwright et al. (2014) for NWA 7034. This model yields 10% uncertainties for the calculated production rates if the pre-atmospheric radius, shielding depth, and chemical composition (Table 2) are known, and if the object is spherical.

For direct comparison of cosmogenic and trapped gases, we used the same deconvolution end-members as Cartwright et al. (2014): for Ne, we adopt a cosmogenic $(^{20}\text{Ne}/^{22}\text{Ne})_c$ ratio of 0.80, a trapped $(^{20}\text{Ne}/^{22}\text{Ne})_t$ ratio of 10.1, and a trapped $(^{21}\text{Ne}/^{22}\text{Ne})_t$ ratio of 0.03. For Ar, we use a cosmogenic $(^{38}\text{Ar}/^{36}\text{Ar})_c$ ratio of 1.5341, and a trapped $(^{38}\text{Ar}/^{36}\text{Ar})_t$ ratio of 0.238.

RESULTS

The results for He, Ne, and Ar are given in Table 3 and the results for Kr and Xe are given in Tables 4 and 5, respectively.

Helium: For GRV 99027, essentially all He was released at or below 1200°C; the higher temperature steps released less than 7% of the total He. The $^4\text{He}/^3\text{He}$ ratios for all temperature steps are nearly constant and remarkably low, between 3.9 and 4.74, indicating that both ^4He and ^3He are predominantly cosmogenic. For NWA 7906, virtually all (>99.9%) of the He was released at or below 1200°C, with >97% released at 800°C, 2.4% at 1000°C, and the remainder at 1200°C. The $^4\text{He}/^3\text{He}$ ratios for the 800°C, 1000°C, and 1200°C temperature steps are 340, 387, and 378, respectively. At higher temperatures, the blank obscures any discussion of $^4\text{He}/^3\text{He}$ ratios. The paired meteorite NWA 7907 exhibits similar He release characteristics as NWA 7906, with >97% of all helium released at 800°C, 2.1% at 1000°C, and the remainder at 1200°C. The $^4\text{He}/^3\text{He}$ ratios for the three temperature steps are 460, 430, and 270.

Neon: For GRV 99027, most of the Ne was released at or below 1400°C, with ~60% of the total Ne released in the 1400°C temperature step. Neon released above 1400°C contributes only ~6% to the total. The Ne isotope ratios are remarkably constant for the different temperature steps. The low $^{20}\text{Ne}/^{22}\text{Ne}$ ratios between 0.72 and 0.83 clearly indicate that measured Ne is predominantly cosmogenic. However, the low $^{21}\text{Ne}/^{22}\text{Ne}$ ratios in the range 0.75-0.79 (excluding the 1740°C step) indicate contributions from solar cosmic rays (see discussion below). NWA 7906 released the vast majority (~95%) of its Ne at or below 1200°C. About 55% of the Ne was released at 800°C and the sample was essentially degassed (for Ne) at 1400°C. The $^{20}\text{Ne}/^{22}\text{Ne}$ and $^{21}\text{Ne}/^{22}\text{Ne}$ ratios range from 0.77-1.30 and 0.80 – 0.85, respectively, for Ne released between 800°C and 1400°C and are clear indicators of irradiation by galactic cosmic rays (GCRs). In fact, there are effectively no indications of either a trapped Ne component and/or contributions from SCR. The release pattern for NWA 7907 is very similar to that of NWA 7906. About 54% of all Ne was released at 800°C, ~99% of the total Ne was released at or below 1200°C, and the sample was essentially degassed at 1400°C. Neon released at higher temperatures made up less than 1‰ of the total. As with NWA 7906, the $^{20}\text{Ne}/^{22}\text{Ne}$ (0.82-0.95) and $^{21}\text{Ne}/^{22}\text{Ne}$ (0.81-0.94) ratios of NWA 7907 indicate that the released Ne is essentially entirely from GCR irradiation with no or only very minor contributions from trapped Ne and/or SCRs.

Argon: The results for GRV 99027 indicate two major ^{36}Ar releases; ~30% of total ^{36}Ar is released in the 1000°C step and ~40% is released in the 1400°C step. Only ~5% of the total ^{36}Ar is released above 1400°C. The $^{38}\text{Ar}/^{36}\text{Ar}$ ratios are in the range 0.199-0.769, indicating that Ar is a mixture of trapped and cosmogenic. 50% of ^{40}Ar is released at 1400°C and 25% is released at 1000°C. The sample was almost completely degassed after the 1600°C temperature step. NWA 7906 released an unexpectedly high concentration of ^{40}Ar at 800°C, going so far as to overcharge the digital voltmeter (DVM) of the Faraday Cup detector. Since the Ar measurements had to be corrected for incompletely separated Ar in the Kr-Xe phase and since this correction is done via ^{40}Ar , it was not possible to determine the total Ar concentration for NWA 7906. The reported ^{36}Ar value in Table 3 is a lower limit, does not account for incomplete separation, and is not used in other calculations. Typically, 10% or less of the total Ar inventory is present in the Kr-Xe phase due to incomplete separation. To avoid such problems in the future, the Ar phases for all later measurements were diluted before being introduced into the mass spectrometer. Of the remaining ^{36}Ar and ^{38}Ar in NWA 7906 and for all ^{36}Ar and ^{38}Ar in NWA 7907, 97% was released at or below 1200°C. For NWA 7906 and NWA 7907, the $^{38}\text{Ar}/^{36}\text{Ar}$ ratios range from 0.184-1.574, showing that Ar in both meteorites is a mixture of trapped and cosmogenic. Most of the ^{40}Ar in NWA 7907 was released at the lowest temperature step at 800°C; releases at higher temperature steps contributed only about 20% to total ^{40}Ar .

Krypton and xenon: GRV 99027 released all its ^{84}Kr and ^{132}Xe at or below 1400°C, with ~40% of each isotope released at 1400°C. As mentioned above, due to technical problems with the spectrometer, we were unable to measure some of the Kr and Xe isotopes for certain temperature steps. Therefore, ^{129}Xe data is available only for the 800°C temperature step, where the $^{84}\text{Kr}/^{132}\text{Xe}$ and $^{129}\text{Xe}/^{132}\text{Xe}$ ratios are 2.05 and 1.100, respectively. In this temperature step, the measured Kr and Xe content appears to be Martian interior with essentially no contribution from either the Martian or terrestrial atmosphere (though it may also be elementally fractionated air – “EFA”, see below). For NWA 7906, the bulk of the Kr and Xe was released at low temperatures; 52% of ^{84}Kr and 59% of ^{132}Xe , respectively, were released at 800°C. The release pattern for NWA 7907 is similar: 59% of ^{84}Kr and 70% of ^{132}Xe were released at 800°C. For both meteorites NWA 7906 and NWA 7907, the $^{129}\text{Xe}/^{132}\text{Xe}$ and $^{84}\text{Kr}/^{132}\text{Xe}$ ratios indicate that Kr and Xe are primarily Martian interior (see below).

Cosmic Ray Exposure Histories

Total isotope ratios were calculated using the summed concentrations of each component for temperature steps where both components were measurable. The cosmogenic $^{21}\text{Ne}_c$ and $^{38}\text{Ar}_c$ concentrations and the $(^{22}\text{Ne}/^{21}\text{Ne})_c$ ratios for the total samples are listed in Table 3.

Diffusive losses

Comparing the measured data with the models indicates minimal ^3He deficits for GRV 99027, with ~30% loss for NWA 7906 and ~40% loss for NWA 7907. This is also reflected in the CRE ages (Table 6), with the ^3He age for GRV 99027 being within 8% of its ^{21}Ne age, while the ^3He ages for NWA 7906 and NWA 7907 are 35% and 40% less than their respective ^{21}Ne ages.

Cosmic ray exposure ages

Cosmic ray exposure history for GRV 99027: The $^4\text{He}/^3\text{He}$ ratio of 4.42 calculated for the total (Table 3) is close to the average volume weighted cosmogenic production rate ratio of 2.96 determined using the model of Leya and Masarik (2009) extended to small shergottites (see following paragraph), with both the measured and modeled ratios being lower than the cosmogenic $^4\text{He}/^3\text{He}$ ratio of ~6 (Wieler 2002 and references therein) for stony meteorites. It is, therefore, safe to assume that all ^3He is cosmogenic, i.e., $^3\text{He}_c$.

For most studies of cosmic ray exposure histories, $(^{22}\text{Ne}/^{21}\text{Ne})_c$ serves as a shielding indicator. However, the high $(^{22}\text{Ne}/^{21}\text{Ne})_c$ ratio of 1.299, although within the uncertainty of the volume weighted average production rate ratio, suggests that some of the cosmogenic Ne is produced by SCR since such a high ratio cannot result from GCR-produced Ne alone except in the outermost centimeter according to the (extended) Leya and Masarik (2009) model. However, the outermost layers are the most likely to be ablated away during atmospheric entry. This finding confirms an earlier study by Garrison et al. (1995) and a recent systematic investigation by Wieler et al. (2016), who both conclude that a sizeable

fraction of the shergottites appears to contain SCR-produced Ne. Consequently, uncorrected CRE ages would be too high since they would treat both SCR and GCR components as being GCR produced. To investigate, we estimated the pre-atmospheric size of GRV 99027 and calculated the ^3He and ^{21}Ne production rates. From the meteorite's found mass of ~ 10 g and post-atmospheric dimensions of $2.2 \times 2.5 \times 2.8$ cm (Lin et al. 2003), we can approximate the meteorite as a (post-atmospheric) sphere of radius ~ 1.25 cm. *First*, assuming there was no explosion at high altitudes, i.e., assuming GRV 99027 was not part of a much larger body and, *second*, assuming $\sim 85\%$ ablation losses (e.g., Bhandari et al. 1980), we estimate the pre-atmospheric radius to be ~ 2.4 cm. The size is remarkably small for Martian meteorites. However, the consistency of the results (see below) gives confidence in the assumptions and the used procedure. For the following discussion, we use the model predictions of Leya and Masarik (2009, extended) with a pre-atmospheric radius of 3 cm to compute volume weighted average production rates using only shielding depths deeper than 1.4 cm below the pre-atmospheric surface, i.e., assuming the found piece is the innermost 15% (by mass) of the entire meteorite. Using the bulk chemical composition given by Lin et al. (2008) (shown in Table 2) as an input to the Leya and Masarik (2009) small shergottite model, we calculated a volume weighted average $(^{22}\text{Ne}/^{21}\text{Ne})_{\text{GCR}}$ ratio of 1.290, a $^{21}\text{Ne}_{\text{GCR}}$ production rate ($P_{21\text{-GCR}}$) of 0.157×10^{-8} $\text{cm}^3 \text{STP}/(\text{g Ma})$, a $^3\text{He}_{\text{GCR}}$ production rate ($P_{3\text{-GCR}}$) of 1.283×10^{-8} $\text{cm}^3 \text{STP}/(\text{g Ma})$, and a $^{38}\text{Ar}_{\text{GCR}}$ production rate ($P_{38\text{-GCR}}$) of 0.030×10^{-8} $\text{cm}^3 \text{STP}/(\text{g Ma})$.

To determine SCR-produced contributions, we use the model of Trappitsch and Leya (2013) model for SCR in micrometeorites (or other small particles), assuming the total fluence of primary particles $J_0 = 100 \text{ cm}^{-2} \text{ s}^{-1}$, the characteristic rigidity of the spectrum $R_0 = 125 \text{ MV}$, and a solar distance of 1 AU. This model over-estimates the production of SCR produced nuclides in GRV 99027 for several reasons: (1) Mars orbits the sun further than the 1 AU distance used in the model, (2) the model assumes negligible shielding (i.e., it is for micrometeorites and interstellar dust particles). Qualitatively, Fig. 3 of Trappitsch and Leya (2014) shows the SCR induced production rate dropping by about an order of magnitude when going from the surface to $\sim 1 \text{ g cm}^{-2}$, which corresponds to a shielding depth of ~ 0.3 cm, with the SCR induced production rate rapidly dropping with increasing depth. As such, the SCR values calculated below are an upper limit.

Using this model, we determine the $(^3\text{He}/^{21}\text{Ne})_{\text{SCR}}$ and $(^{38}\text{Ar}/^{21}\text{Ne})_{\text{SCR}}$ ratios (Table 6) and find that <1% of the ^3He is produced by SCR. Comparing the measured cosmogenic $(^{22}\text{Ne}/^{21}\text{Ne})_{\text{c}}$ ratio of 1.299 with the modelled $(^{22}\text{Ne}/^{21}\text{Ne})_{\text{GCR}}$ ratio of 1.290 and using the modeled SCR produced $(^{22}\text{Ne}/^{21}\text{Ne})_{\text{SCR}}$ ratio of 1.397 and the bulk chemical composition of Lin et al. (2008), we calculate that up to ~10% of the measured Ne is produced by SCR. Since ^{38}Ar is composed of a mixture of cosmogenic (i.e., GCR and SCR produced) and unknown trapped components including, potentially, Martian atmosphere, Martian interior, air, EFA, and other components, we cannot use this method to quantify the amount of GCR and SCR produced ^{38}Ar .

If we assume that T_{38} is equal to the average of T_3 and T_{21} , we can multiply T_{38} and $P_{38\text{-GCR}}$ to determine the amount of $^{38}\text{Ar}_{\text{GCR}}$. Since we know the $(^{38}\text{Ar}/^{21}\text{Ne})_{\text{SCR}}$ ratio and $^{21}\text{Ne}_{\text{SCR}}$ (Table 6), we can determine the amount of $^{38}\text{Ar}_{\text{SCR}}$. Subtracting $^{38}\text{Ar}_{\text{GCR}}$ from the total yields a “leftover” mix of unknown trapped components (including SCR), with the “leftover” mix comprising about 38% of the total ^{38}Ar . If, in addition, we subtract the calculated $^{38}\text{Ar}_{\text{SCR}}$, the “leftover” mix makes up about 21% of the total ^{38}Ar . Using the same method with ^{36}Ar and its GCR and SCR production rates (Table 6) instead of ^{38}Ar we calculate that the “leftover” mix including SCR comprises about 90% of the total ^{36}Ar , while the “leftover” mix after subtracting SCR comprises about 89% of the total ^{36}Ar inventory.

Using now the volume averaged ^3He and ^{21}Ne production rates (see above) and GCR-produced ^3He , ^{21}Ne (corrected for SCR contributions), we calculate ^3He and ^{21}Ne cosmic ray exposure ages of $T_3 = 5.4$ Ma and $T_{21} = 5.4$ Ma. Since these ages lie within the 10% uncertainty of the CRE ages calculated without considering SCR corrections ($T_3 = 5.5$ Ma, $T_{21} = 5.9$ Ma, $T_{\text{avg}} = 5.7$ Ma. See Table 6.) and the calculated SCR contributions represent an upper limit, we consider the potential SCR contribution to be not very significant and so adopt the GCR-only CRE ages. The lack of ^{36}Ar data for the 1740°C temperature means we cannot deconvolve ^{36}Ar and ^{38}Ar , and so cannot determine the total cosmogenic ^{38}Ar concentration or the ^{38}Ar CRE age (T_{38}). The finding that T_3 and T_{21} are consistent with each other despite the different magnitudes of corrections for SCR contributions confirms our procedure and gives confidence in the data.

Our adopted noble gas CRE age for GRV 99027 is ~29% greater than the 4.4 ± 0.6 Ma CRE age determined by Kong et al. (2007) based on ^{10}Be data and a now-obsolete ^{10}Be half-life of 1.51 Ma. We expect that this discrepancy is most likely due to differing estimates of shielding depth and, therefore, of the ^{10}Be saturation activity. In addition, a significant terrestrial age can result in the ^{10}Be age being shorter than the noble gas CRE age. Using the updated ^{10}Be half-life of 1.387 ± 0.012 Ma (Korschinek et al. 2010), the Kong et al. (2007) age drops to 4.1 Ma, though it is unclear which ^{10}Be standard they used, how it was defined, and how the half-life of the standard is used in the definition, so the reliability of this age is not known to us.

Using the extended production rate model of Leya and Masarik (2009) for noble gases in small shergottites as well as an additional expansion of the same model to ^{10}Be (and assuming 10% uncertainty in the calculated production rates), our measured cosmogenic $(^{22}\text{Ne}/^{21}\text{Ne})_c$ ratio of 1.299, the bulk chemical composition of Lin et al. (2008), the present activity of ^{10}Be in GRV 99027 (14.1 ± 0.6 dpm/kg, Kong et al. 2007), and the old 1.51 Ma half-life for ^{10}Be , we calculate the ^{10}Be saturation activity to be 15.9 dpm/kg and further calculate a CRE age of 4.8 ± 2.0 Ma, i.e., within the uncertainties identical to the adopted noble gas CRE age. The uncertainty in our calculated ^{10}Be CRE age is larger than that of Kong et al. (2007) because we assigned and propagated a 10% uncertainty to the modeled ^{10}Be saturation activity, while Kong et al. (2007) did not consider any uncertainty. To bring the calculated ^{10}Be CRE age more in line with our adopted noble gas CRE age of 5.7 Ma, a terrestrial age of ~90 ka would be needed. Note, if we use the bulk chemistry reported by Kong et al. (2007) instead, we calculate the ^{10}Be saturation activity to be 15.7 dpm/kg and a CRE age of 4.9 ± 2.0 Ma.

For purposes of comparison, the results of which can be seen in Fig. 1 and Table 6, we re-computed the CRE ages for other poikilitic basaltic shergottites (formerly termed lherzolithic shergottites) ALHA77005, LEW88516, Y-793605, and NWA 1950 using the production rate model of Leya and Masarik (2009) extended to small shergottites and the bulk chemical composition from Eugster et al. (2002) for ALHA77005, Lodders (1998) for LEW88516, Warren and Kallemeyn (1997) for Y-793605, and Gillet et al. (2005) for NWA 1950. With the exception of NWA 1950, which Gillet et al. (2005) reported as having a cosmogenic $(^{22}\text{Ne}/^{21}\text{Ne})_c$ ratio of 1.38, the reported cosmogenic $(^{22}\text{Ne}/^{21}\text{Ne})_c$ ratios for the four meteorites are not excessively high (i.e., not >1.25 , see the “SCR Noble Gases in Shergottites

and other Achondrites” section of Wieler et al. 2016), so we assume they were exposed only to GCRs and the $(^{22}\text{Ne}/^{21}\text{Ne})_c$ ratio can be used as a proxy for shielding depth. Due to the likely presence of SCR in the NWA 1950 sample measured by Gillet et al. (2005), we exclude this sample from the comparison and instead use the noble gas data reported by Christen et al. (2005) for NWA 1950 since their sample has a cosmogenic $(^{22}\text{Ne}/^{21}\text{Ne})_c$ ratio of 1.249. For all meteorites used in this comparison (i.e., GRV 99027, ALHA77005, Y-793605, LEW88516, and NWA 1950), the CRE ages calculated using the production rates from Leya and Masarik (2009) for ordinary chondrites are, on average, ~1.5 Ma older than the ages reported by Eugster et al. (1997), Terribilini et al. (1998), Gillet et al. (2005), and Christen et al. (2005); all of them used the production rate systematics of Eugster and Michel (1995). Both the originally reported and re-calculated ages are shown in Table 6. In their study of 18 Martian shergottites, Wieler et al. (2016) measured a systematic offset as well, with the Leya and Masarik (2009) model yielding older CRE ages; the standard deviation of the difference between their preferred ages (T_{mean}) and the ^{21}Ne ages computed using the Eugster and Michel (1995) systematics ($T_{21\text{E\&M}}$) was 1.1 Ma; the average difference was 0.9 Ma. For the four shergottites we used for comparison, the standard deviation of the difference between our calculated T_{mean} and $T_{21\text{E\&M}}$ is 0.6 Ma; the average difference is 1.2 Ma. The reason for this offset may be due to the method of Eugster and Michel (1995) being tailored to howardites, eucrites, and diogenites, along with the assumption that lherzolites are chemically similar to diogenites (Eugster et al. 1997). However, the relative abundance of several key target elements (Mg, Al, Si, and Na) in diogenites differs significantly from those of lherzolites, which may cause the Eugster and Michel (1995) and Leya and Masarik (2009) methods to differ, particularly because the former method requires a type-specific shielding parameter in addition to the bulk chemical composition. In contrast, the Leya and Masarik (2009) method requires only the bulk chemical composition and $(^{22}\text{Ne}/^{21}\text{Ne})_c$ ratio of the sample to calculate $^{21}\text{Ne}_c$ production rates and is not dependent on a type-specific shielding parameter, so we consider it more reliable. The thus-determined T_3 , T_{21} , and T_{38} CRE ages for each meteorite are consistent with each other; therefore, we use the average CRE ages of each meteorite for the discussion. The average ages range from 3.9 – 6.03 Ma (Table 6). For the discussion, we also add the CRE ages of NWA 4797 and NWA 6342 of 5.25 Ma and 5.10 Ma, respectively, from Wieler et al. (2016). The grand average of the re-calculated CRE ages for the seven poikilitic basaltic

shergottites is 5.58 ± 0.13 Ma (Table 6, Fig. 1). The finding of the same exposure ages suggests that all seven poikilitic basaltic shergottites were likely ejected from Mars in a single, common event.

Cosmic ray exposure history for NWA 7906 and NWA 7907: The meteorites NWA 7906 and NWA 7907 are likely paired with each other and with NWA 7034 (Ruzicka et al. 2015). Since Cartwright et al. (2014) analyzed the noble gases in NWA 7034, we can compare our data for NWA 7906 and NWA 7907 to their results. Doing so, we find that a major difference is in the $(^{22}\text{Ne}/^{21}\text{Ne})_c$ ratios; Cartwright et al. (2014) measured for NWA 7034 a ratio of ~ 1.27 while we measured lower $(^{22}\text{Ne}/^{21}\text{Ne})_c$ ratios of 1.212 and 1.196 for NWA 7906 and NWA 7907, respectively. Although our data are very consistent for the two meteorites, and the differences between both studies are $\sim 5\%$, they are nevertheless significant. Since we have no chemical composition data for the basaltic breccias NWA 7906 and 7907 samples we analyzed, the following discussion is based on the bulk chemical data of NWA 7034 (Agee et al. 2013, Table 2). Based on this chemical composition, the model by Leya and Masarik (2009) predicts for all radii and all shielding depths $(^{22}\text{Ne}/^{21}\text{Ne})_c$ ratios higher than measured by us. This can be seen in Fig. 2a (upper panel), where we plot modeled ^{21}Ne production rates as a function of $(^{22}\text{Ne}/^{21}\text{Ne})_c$ for meteorites with a chemical composition of NWA 7034 and pre-atmospheric radii between 10 cm and 85 cm. The pink area indicates the $(^{22}\text{Ne}/^{21}\text{Ne})_c$ ratio of ~ 1.27 measured by Cartwright et al. (2014), while the green and yellow areas indicate the $(^{22}\text{Ne}/^{21}\text{Ne})_c$ ratios measured by us for NWA 7907 and NWA 7906, respectively. Here the difficulty becomes obvious: the lowest modeled $(^{22}\text{Ne}/^{21}\text{Ne})_c$ ratio of 1.251, which is for meteoroids with a radius of 10 cm, is still $\sim 3\%$ higher than the ratios measured by us. In contrast, the higher $(^{22}\text{Ne}/^{21}\text{Ne})_c$ value measured by Cartwright et al. (2014) is well within the range of the modeled ratios. Due to this problem, we cannot straightforwardly use the relationships of ^3He , ^{21}Ne , and ^{38}Ar production rates as a function of $(^{22}\text{Ne}/^{21}\text{Ne})_c$ to determine CRE ages. The most plausible explanation for this discrepancy is chemical inhomogeneity of the samples; a minor change in composition from one aliquot to the next can significantly affect the results. In particular, a small change in the sodium abundance can result in a relatively large change in $(^{22}\text{Ne}/^{21}\text{Ne})_c$ ratios. If we assume that NWA 7034, NWA 7906, and NWA 7907 all originated from a large (>50 cm) meteoroid (Cartwright et al. 2014), assuming of a sodium concentration of $\sim 1.5\text{wt}\%$ for our samples (instead of the 2.8% measured by Agee et al. 2013) brings modeled and measured

$(^{22}\text{Ne}/^{21}\text{Ne})_c$ ratios into agreement. This can be seen in Fig. 2b (lower panel), where we plot $^{21}\text{Ne}_c$ production rates as a function of $(^{22}\text{Ne}/^{21}\text{Ne})_c$ for meteorites with pre-atmospheric radii between 10 cm and 85 cm with a chemical composition otherwise identical to NWA 7034 except for having a lower sodium concentration of 1.5wt%. In this scenario, the $(^{22}\text{Ne}/^{21}\text{Ne})_c$ ratios measured by us for NWA 7907 (green area) and NWA 7906 (yellow area) are possible at larger shielding depths in meteorites with pre-atmospheric radii of ~50 cm.

Assuming relatively large chemical inhomogeneities of the samples is reasonable considering that the host meteorite is classified as a basaltic breccia. Sample heterogeneities are likely due to a heterogeneous distribution of the alkaline basaltic clasts; the fine-grained matrix is most likely more homogeneous, although matrix clasts can also be recognized. The possibility of major chemical inhomogeneities is further confirmed by the detailed study of Humayun et al. (2013), who spot-wise measured the chemical composition of NWA 7533, which is paired with NWA 7034, and found large variations; the measured sodium concentration varied between 0.1wt% and 3.7wt%. While this all sounds reasonable, it is not easy to understand why both of our samples have similar but lower sodium concentrations than the sample measured by Cartwright et al. (2014).

Using the thus-modified chemical composition for NWA 7906 and NWA 7907, assuming a pre-atmospheric radius of 85 cm, using the model of Leya and Masarik (2009) for ordinary chondrites, and using the cosmogenic $(^{22}\text{Ne}/^{21}\text{Ne})_c$ ratio as a proxy for shielding depth, we calculate CRE ages of $T_3 = 4.25$ Ma, $T_{21} = 6.60$ Ma, and $T_{38} = 1.40$ Ma for NWA 7906 and $T_3 = 3.67$ Ma, $T_{21} = 6.08$ Ma, and $T_{38} = 2.60$ Ma for NWA 7907. Assuming the trapped component is Martian atmosphere, as Cartwright et al. (2014) did, we find that T_{38} is significantly lower than T_3 and T_{21} . This discrepancy persists even if we consider air ($^{38}\text{Ar}/^{36}\text{Ar} = 0.1885$, Lee et al. 2006) as the dominant trapped component, with $T_{38\text{-air}}$ ages of 1.73 and 2.83 Ma, respectively, in such a case. Since both meteorites are breccias, we believe it most likely that the discrepancy in CRE ages is due to inhomogeneity in the chemical composition of the meteorites, particularly in light of the likely inhomogeneities discussed above.

Combining the T_3 and T_{21} ages, we calculate very consistent average ages of 5.42 ± 0.39 (1σ) Ma and 4.87 ± 0.35 (1σ) Ma for NWA 7906 and NWA 7907, respectively, which agree well with the CRE age of

~5 Ma favored by Cartwright et al. (2014). Note that the adjustment of the chemical composition, i.e., assuming a lower sodium concentration, affects only T_{21} but not T_3 or T_{38} . We therefore consider the consistency of T_3 and T_{21} ages for not one meteorite but for the two meteorites studied here and the good agreement with the data for NWA 7034 (Cartwright et al. 2014) as a confirmation of our procedure.

Gas Retention Ages

^4He and ^{40}Ar gas retention ages for GRV 99027: Measured Ar is a mixture of different components, which prohibits the straightforward calculation of K- ^{40}Ar gas retention ages. Measured $^{40}\text{Ar}/^{36}\text{Ar}$ ratios for all temperature steps are lower than that of the Martian atmosphere (1900-2400) (e.g., Swindle 2002; Mahaffy et al. 2013; Atreya et al. 2013), which suggests that, in addition to potentially trapped Martian atmosphere and radiogenic ^{40}Ar , a component with a lower $^{40}\text{Ar}/^{36}\text{Ar}$ ratio such as that from the Martian mantle ($^{40}\text{Ar}/^{36}\text{Ar} \leq 200$) (Mathew and Marti 2001) and/or the terrestrial atmosphere ($^{40}\text{Ar}/^{36}\text{Ar} \sim 296$) must be present. Assuming all measured ^{40}Ar to be radiogenic would result in a ^{40}Ar gas retention age of 1.74 ± 0.08 Ga, which we consider unreasonably high, but we have no means of better determining the age.

Calculating the ^4He gas retention age for GRV 99027 is not straightforward because all measured $^4\text{He}/^3\text{He}$ ratios are consistent with cosmogenic, indicating that radiogenic ^4He is low or even absent. To calculate the age, we use the U (9 ppb), Th (31 ppb), and Sm (254 ppb) concentrations measured by Lin et al. (2008) and the U-Th-Sm/ ^4He method (Farley 2002, Zeitler 2015). The upper limit on the ^4He retention age, calculated using the total ^4He concentration, is ~156 Ma. Note that this is not reasonable, as it assumes all ^4He to be radiogenic. A more realistic age is determined by multiplying the cosmogenic $(^4\text{He}/^3\text{He})_c$ ratio from the average volume weighted production rates with shielding depths deeper than 1.4 cm from the surface as described above (i.e., 2.956) by the measured total ^3He to determine the concentration of cosmogenic ^4He , which is then subtracted from the total amount of ^4He for which both ^3He and ^4He have been measured. The thus-determined ^4He retention age of ~54 Ma suggests partial degassing. Within this range of shielding depths, the modeled cosmogenic $^4\text{He}/^3\text{He}$ ratio ranges from

2.900 at 3.047, which result in ^4He retention ages of 55 and 51 Ma, respectively, so we consider the ~54 Ma retention age calculated using the volume-weighted average ratio to be reasonable.

The upper limit to the ^4He retention age is much lower than the Rb-Sr age (177 ± 5 Ma) reported by Liu et al. (2011) for GRV 99027 and the concordant Rb-Sr and Sm-Nd ages for other shergottites (~180 Ma) reported by Shih et al. (1982); however, this may be reasonable considering that this meteorite is heavily shocked and experienced slow cooling (Wang and Chen 2006). Note that there is still some debate over the crystallization ages for shergottites: a high crater density indicating an “old” Martian surface and Pb-Pb isochron ages older than 4 Ga (e.g., Bouvier et al. 2008, 2009) contrast with “young” radiometric mineral isochrons, e.g., Sm-Nd and Rb-Sr (Liu et al. 2011). It is not yet understood whether this discrepancy is due to reset of the isochrons by alteration (Bouvier et al. 2005) and/or by impacts (Bouvier et al. 2008).

Gas retention ages for NWA 7906: Unfortunately we cannot determine the ^{40}Ar gas retention age for NWA 7906 because we have no ^{40}Ar data for the 800°C temperature step due to our accidentally overcharging the DVM. Based on measured ^4He concentrations and the elemental U, Th, and Sm abundances of 0.51, 2.64, and 6.433 ppm, respectively, in NWA 7034 (Agee et al. 2013) we calculate a U-Th-Sm/He age of ~165 Ma, which is in good agreement with the ~170 Ma age reported by Cartwright et al. (2014). Assuming the same 1.27 ± 0.17 (1σ) Ga ^{40}Ar retention age as NWA 7907 (see below), the data indicate that ~88% of the radiogenic ^4He has been lost.

Gas retention ages for NWA 7907: We assume that all ^{40}Ar in NWA 7907 was produced by in situ decay of ^{40}K . Using the decay constant of Steiger and Jäger (1977) and a potassium abundance of 2800 ppm in NWA 7034 (Agee et al. 2013), we find an upper limit for the ^{40}Ar retention age of 1.27 ± 0.17 (1σ) Ga. The age is in good agreement with the 1.56 Ga retention age found by Cartwright et al. (2014) and is also consistent with the U-Pb zircon age of 1.7 Ga (Humayun et al. 2013). Using the measured ^4He concentration and the elemental U, Th, and Sm abundances of 0.51, 2.64, and 6.433 ppm, respectively, (Agee et al. 2013), we calculate a U-Th/He age of ~194 Ma, in good agreement with the ^4He gas retention age for NWA 7906 (see above) and also in agreement with the ~170 Ma age reported by Cartwright et al. (2014). Assuming the same retention ages for ^4He and ^{40}Ar , we calculate that ~86%

of the radiogenic ^4He has been lost, clearly indicating a late disturbance of the U-Th- ^4He age, possibly during meteoroid ejection from Mars.

Trapped components

Figure 3 shows $^{129}\text{Xe}/^{132}\text{Xe}$ ratios as a function of $^{84}\text{Kr}/^{132}\text{Xe}$ ratios. In addition to the experimental values, we show data for Martin Interior (MI; Ott 1988), Earth Atmosphere (EA; Pepin et al. 1995, Swindle 2002), Martian atmosphere (nakhlites & ALH 84001) (“MANA”; Mathew and Marti 2001, Swindle 2002, Wieler et al. 2016), and Martian atmosphere (shergottites) (“MAS”; Bogard and Garrison 1998, Swindle 2002, Wieler et al. 2016). For comparison, we also plot data for shergottites (Bogard and Garrison 1998; Llorca et al. 2013; Mathew et al. 2003) and NWA 7034 (Cartwright et al. 2014).

Trapped components in GRV 99027: We have only very limited Xe data for the discussion of trapped components. However, the data for the 800°C step indicates that trapped Kr and Xe are almost exclusively from the Martian interior (large diamond in Fig. 3). Other shergottites shown in Fig. 3 also have $^{129}\text{Xe}/^{132}\text{Xe}$ and $^{84}\text{Kr}/^{132}\text{Xe}$ ratios that cluster around the values for Martian interior, though some (also) contain Martian and/or terrestrial atmosphere. Mohapatra et al. (2009) and Schwenzer et al. (2009) stated that low-temperature releases (i.e., <1000°C for hot desert finds, potentially higher for Antarctic finds) from Martian meteorites can also be contaminated with elementally fractionated air (EFA). The Ar, Kr, and Xe signatures of EFA are indistinguishable from those of Chassigny/Martian interior. However, due to the possible presence of EFA, and the limited Kr and Xe data for GRV 99027 (see above), it is not possible to put better constraints on the trapped component(s).

Trapped components in NWA 7906 and NWA 7907: The $^{129}\text{Xe}/^{132}\text{Xe}$ and $^{84}\text{Kr}/^{132}\text{Xe}$ ratios for these two meteorites are mixtures that may comprise Martian interior, EFA, and possibly also some Martian atmosphere (Fig. 3). Since NWA 7906 and 7907 (together with NWA 7034) have old crystallization ages (~4.4 Ga, Cartwright et al. 2014 and references therein) but have a disturbance in the ^{40}Ar and U-Pb retention ages at ~1.7 Ga (Cartwright et al. 2014 and references therein), we may expect more

Martian atmosphere, in comparison to GRV 99027, to be incorporated into the meteoroids. However, this is not observed due to the likely presence of EFA in these samples and the insufficiency of our measured data to constrain the ^{40}Ar retention age of GRV 99027.

Summary and Conclusion

We measured the isotopic concentrations of He, Ne, Ar, Kr, and Xe in the poikilitic basaltic shergottites GRV 99027 and the paired basaltic breccias NWA 7906 and NWA 7907. Using the updated version of the production rate model of Leya and Masarik (2009) tailored specifically for small shergottites for GRV 99027 and the original model with ordinary chondrite systematics for NWA 7906 and NWA 7907, we calculated CRE ages of 5.70 ± 0.40 Ma, 5.42 ± 0.39 Ma, and 4.87 ± 0.35 Ma for GRV 99027, NWA 7906, and NWA 7907, respectively. For GRV 99027, there are indications of contributions from solar cosmic rays, which is consistent with a small pre-atmospheric size and which is often seen for meteorites from rare classes (Wieler et al. 2016). We re-calculated CRE ages for other poikilitic basaltic shergottites using literature noble gas data and the updated production rates. The thus-determined consistent CRE ages for seven poikilitic basaltic shergottites are consistent within the uncertainties, indicating that all of them were likely ejected in the same event 5.58 ± 0.25 Ma ago.

A comparison of our data for NWA 7906 and NWA 7907 to the data determined for the paired specimen NWA 7034 by Cartwright et al. (2014) is difficult because all are basaltic breccias, and the chemical composition upon which we base our CRE age calculations can be highly variable over small sample sizes. However, slightly decreasing the sodium concentration of NWA 7906 / NWA 7907 relative to NWA 7034, and assuming that all originated from a large (>50cm diameter) meteoroid, the CRE ages for all three meteorites agree to be ~5 Ma.

The upper limit of the ^4He gas retention age for GRV 99027 is ~156 Ma but this unreasonably assumes all ^4He to be radiogenic; the more realistic value of ~54 Ma, estimated from the cosmogenic $(^4\text{He}/^3\text{He})_c$ ratio, suggests partial loss of ^4He . This lower age is much lower than Rb-Sr and Sm-Nd ages for GRV 99027 (Liu et al. 2011) and other shergottites (Shih et al. 1982), though this may be reasonable (see text above). Due to technical problems, we were unable to calculate a ^{40}Ar gas retention age for NWA 7906, though our ^4He retention age of ~165 Ma is in good agreement with the ~170 Ma age

reported by Cartwright et al. (2014). The ^{40}Ar gas retention age for NWA 7907 of ~ 1.3 Ga is consistent with findings from Cartwright et al. (2014) and with the U-Pb zircon age of ~ 1.7 Ga obtained by Humayun et al. (2013). The ^4He retention age of ~ 194 Ma agrees well with Cartwright et al. (2014) for the paired meteorite NWA 7034. The ^4He gas retention ages for NWA 7906 and 7907 in the range 200 Ma indicate that about 90% of the radiogenic ^4He have been lost.

Heavy noble gas (Kr, Xe) data for all three meteorites reveals that GRV 99027 is composed mainly of Martian interior, while NWA 7906 and NWA 7907 are mixtures that contain Martian interior, EFA, and possibly some Martian atmosphere. However, the presence of EFA, which is indistinguishable from Martian interior, may mask the Martian gases at the temperature steps for which we have data.

Acknowledgements

The authors would like to thank Patrick Enderli and Hans-Erich Jenni for their tireless work in keeping the mass spectrometer laboratory working, and Susanne Schwenzer for the extremely informative discussion regarding elementally fractionated air. Additionally, we would like to thank Gregory Herzog, Uli Ott, and Rainer Wieler, for their detailed and helpful reviews, and Marc Caffee for his editorial handling. This work was supported by the Swiss National Science Foundation (SNF) and the Natural Science Foundation of China (41430105).

REFERENCES

- Agee C. B., Wilson N. V., McCubbin F. M., Ziegler K., Polyak V. J., Sharp Z. D., Asmerom Y., Nunn M. H., Shaheen R., Thiemens M. H., Steele A., Fogel M. L., Bowden R., Glamoclija M., Zhang Z. and Elardo, S. M. 2013. Unique meteorite from early Amazonian Mars: Water-rich basaltic breccia Northwest Africa 7034. *Science* 339(6121):780-785.
- Atreya S. K., Trainer M. G., Franz H. B., Wong M. H., Manning H. L. K., Malespin C. A., Mahaffy P. R., Conrad P. G., Brunner A. E., Leshin L. A., Jones J. H., Webster C. R., Owen T. C., Pepin R. O., & Navarro - González, R. 2013. Primordial argon isotope fractionation in the atmosphere of Mars measured by the SAM instrument on Curiosity and implications for atmospheric loss. *Geophysical Research Letters* 40(21):5605-5609.
- Bhandari N., Lal D., Rajan R. S., Arnold J. R., Marti K., and Moore C. B. 1980. Atmospheric ablation in meteorites: A study based on cosmic ray tracks and neon isotopes. *Nuclear Tracks* 4:213-262.
- Bogard D. D., and Garrison D. H. 1998. Relative abundances of argon, krypton, and xenon in the Martian atmosphere as measured in Martian meteorites. *Geochimica et Cosmochimica Acta* 62(10):1829-1835.
- Bouvier A., Blichert-Toft J., Vervoort J. D., and Albarède F. 2005. The age of SNC meteorites and the antiquity of the Martian surface. *Earth and Planetary Science Letters* 240:221-233.
- Bouvier A., Blichert-Toft J., Vervoort J. D., Gillet P., and Albarède F. 2008. The case for old basaltic shergottites. *Earth and Planetary Science Letters* 266:105-124.
- Bouvier A., Blichert-Toft J., and Albarède F. 2009. Martian meteorite chronology and the evolution of the interior of Mars. *Earth and Planetary Science Letters* 280:285-295.
- Bridges J. C., and Warren P. H. 2006. The SNC meteorites: basaltic igneous processes on Mars. *Journal of the Geological Society* 163:229-251.
- Cartwright J. A., Ott U., Herrmann S., and Agee C. B. 2014. Modern atmospheric signatures in 4.4 Ga Martian meteorite NWA 7034. *Earth and Planetary Science Letters* 400:77-87.

- Christen F., Eugster O., and Busemann H. 2005. Mars ejection times and neutron capture effects of the nakhlites Y000593 and Y000749, the olivine-phyric shergottite Y980459, and the Iherzolite NWA1950. *Antarctic Meteorite Research* 18:117-132.
- Dalcher N., Caffee M. W., Nishiizumi K., Welten K. C., Vogel N., Wieler R., and Leya I. 2013. Calibration of cosmogenic noble gas production in ordinary chondrites based on ^{36}Cl - ^{36}Ar ages. Part 1: Refined produced rates for cosmogenic ^{21}Ne and ^{38}Ar . *Meteoritics & Planetary Science* 48:1841-1862.
- Eugster O., and Michel Th. 1995. Common asteroid break-up events of eucrites, diogenites, and howardites and cosmic-ray production rates for noble gases in achondrites. *Geochimica et Cosmochimica Acta* 59(1):177-199.
- Eugster O., Weigel A., and Polnau E. 1997. Ejection times of Martian meteorites. *Geochimica et Cosmochimica Acta* 61(13):2749-2757.
- Eugster O., Busemann H., Lorenzetti S., and Terribilini D. 2002. Ejection ages from krypton-81-krypton-83 dating and pre-atmospheric sizes of martian meteorites. *Meteoritics & Planetary Science* 37:1345-1360.
- Farley K. 2002. (U-Th)/He Dating: Techniques, Calibrations, and Applications. In *Reviews in Mineralogy and Geochemistry*, Vol. 47, edited by Porcelli D., Ballentine C. J., and Wieler R. Washington (D.C.): Mineralogical Society of America. pp. 819-844.
- Garrison D. H., Rao M. N., and Bogard D. D. 1995. Solar-proton-produced neon in shergottite meteorites and implications for their origin. *Meteoritics* 30:738-747.
- Gillet P., Barrat J. A., Beck P., Marty B., Greenwood R. C., Franchi I. A., Bohn M., and Cotten J. 2005. Petrology, geochemistry, and cosmic - ray exposure age of Iherzolithic shergottite Northwest Africa 1950. *Meteoritics & Planetary Science* 40(8):1175-1184.
- Herzog G. F. and M. W. Caffee. 2014. Cosmic-ray exposure ages of meteorites. In *Volume 1 of Treatise on Geochemistry*, 2nd ed., edited by Holland H. D., and Turekian K. K. Oxford: Elsevier. pp. 419-454.

- Humayun M., Nemchin A., Zanda B., Hewins R. H., Grange M., Kennedy A., Lorand J.-P., Göpel C., Fieni C., Pont S. and Deldicque D. 2013. Origin and age of the earliest Martian crust from meteorite NWA 7533. *Nature* 503(7477):513-516.
- Irving A. J., Kuehner S. M., Lapen T. J., Richter M., Busemann H., Wieler R., and Nishiizumi K. 2017. Keeping up with the Martian meteorites and constraining the number of separate launch sites on Mars (abstract #2068). 48th Lunar and Planetary Science Conference.
- Jagoutz E. 1989. Sr and Nd isotopic systematics in ALHA 77005: Age of shock metamorphism in shergottites and magmatic differentiation on Mars. *Geochimica et Cosmochimica Acta* 53(9):2429-2441.
- Kong P, Fabel D., Brown R., and Freeman S. 2007. Cosmic-ray exposure age of Martian meteorite GRV 99027. *Science in China Series D: Earth Sciences* 50(10):1521-1524.
- Korschinek G., Bergmaier A., Faestermann T., Gerstmann U. C., Knie K., Rugel G., Wallner A., Dillmann I., Dollinger G., Lierse von Gostomski Ch., Kossert K., Maiti M., Poutivtsev M., and Remmert A. 2010. A new value for the half-life of ^{10}Be by Heavy-Ion Elastic Recoil Detection and liquid scintillation counting. *Nuclear Instruments and Methods in Physics Research Section B: Beam Interactions with Materials and Atoms* 268:187-191.
- Lee J-Y., Marti K., Severinghaus J. P., Kawamura K., Yoo H.-S., Lee J. B., and Kim J. S. 2006. A redetermination of the isotopic abundances of atmospheric Ar. *Geochimica et Cosmochimica Acta* 70:4507-4512.
- Leya I., and Masarik J. 2009. Cosmogenic nuclides in stony meteorites revisited. *Meteoritics & Planetary Science* 44(7):1061-1086.
- Lin Y., Wang D., Miao B., Ouyang Z., Liu X., and Ju Y. 2003. Grove Mountains (GRV) 99027: A New Martian meteorite, *Chinese Science Bulletin* 48(16):1771-1774.
- Lin Y., Guan Y., Wang D., Kimura M., and Leshin L. A. 2005. Petrogenesis of the new Iherzolitic shergottite Grove Mountains 99027: Constraints of petrography, mineral chemistry, and rare earth elements. *Meteoritics & Planetary Science* 40(11):1599-1619.

- Lin Y., Qi L., Wang G., and Xu L. 2008. Bulk chemical composition of Iherzolitic shergottite Grove Mountains 99027—Constraints on the mantle of Mars. *Meteoritics & Planetary Science* 43(7):1179-1187.
- Liu T., Li C., and Lin Y. 2011. Rb - Sr and Sm - Nd isotopic systematics of the Iherzolitic shergottite GRV 99027. *Meteoritics & Planetary Science* 46(5):681-689.
- Llorca J., Roszjar J., Cartwright J.A., Bischoff A., Ott U., Pack A., Merchel S., Rugel G., Fimiani L., Ludwig P., Casado J.V., and Allepuz D. 2013. The Ksar Ghilane 002 shergottite – The 100th registered Martian meteorite fragment. *Meteoritics & Planetary Science*. 48(3):493–513.
- Lodders K. 1998. A survey of shergottite, nakhlite and chassigny meteorites whole - rock compositions. *Meteoritics & Planetary Science* 33(S4):A183-A190.
- Mahaffy P. R., Webster C. R., Atreya S. K., Franz H., Wong M., Conrad P. G., Harpold D., Jones J. J., Leshin L. A., Manning H., Owen T., Pepin R. O., Squyres S., Trainer M., and MSL Science Team. 2013. Abundance and isotopic composition of gases in the Martian atmosphere from the Curiosity rover. *Science* 341(6143):263-266.
- Marty B., Heber V. S., Grimberg A., Wieler R., and Barrat J-A. 2006. Noble gases in the Martian meteorite Northwest Africa 2737: A new chassignite signature. *Meteoritics & Planetary Science* 41(5):739-748.
- Mathew K. J., and Marti K. 2001. Early evolution of Martian volatiles: Nitrogen and noble gas components in ALH84001 and Chassigny. *Journal of Geophysical Research: Planets* 106(E1):1401-1422.
- Mathew K.J., Marty B., Marti K., and Zimmermann L. 2003. Volatiles (nitrogen, noble gases) in recently discovered SNC meteorites, extinct radioactivities and evolution. *Earth and Planetary Science Letters* 214(1–2):27-42.

- Mohapatra R., Schwenger S., Herrmann S., Murty S., Ott U., and Gilmour J. 2009. Noble gases and nitrogen in Martian meteorites Dar al Gani 476, Sayh al Uhaymir 005 and Lewis Cliff 88516: EFA and extra neon. *Geochimica et Cosmochimica Acta* 73:1505-1522.
- Nishiizumi K., Regnier S., and Marti K. 1980. Cosmic ray exposure ages of chondrites, pre-irradiation and constancy of cosmic ray flux in the past. *Earth and Planetary Science Letters* 50:156-170.
- Ott, U. 1988. Noble gases in SNC meteorites: Shergotty, Nakhla, Chassigny. *Geochimica et Cosmochimica Acta* 52(7):1937-1948.
- Pepin R. O., Becker R. H., and Rider P. E. 1995. Xenon and krypton isotopes in extraterrestrial regolith soils and in the solar wind. *Geochimica et Cosmochimica Acta* 59(23):4997-5022.
- Ruzicka A., Grossman J., Bouvier A., Herd C. D. K., and Agee C. B. 2015. The Meteoritical Bulletin, No. 102. *Meteoritics & Planetary Science* 50:1662.
- Schwenger S., Herrmann S., and Ott U. 2009. Noble gases in two shergottites and one nakhlite from Antarctica: Y000027, Y000097, and Y000593. *Polar Science* 3:83-99.
- Shih C.-Y., Nyquist L. E., Bogard D. D., McKay G. A., Wooden J. L., Bansal B. M., and Wiesmann H. 1982. Chronology and petrogenesis of young achondrites, Shergotty, Zagami, and ALHA77005: late magmatism on a geologically active planet. *Geochimica et Cosmochimica Acta* 46:2323-2344.
- Steiger R., and Jäger E. 1977. Subcommittee on geochronology: convention on the use of decay constants in geo- and cosmochronology. *Earth and Planetary Science Letters* 36(3):359-362.
- Swindle T. D. 2002. Martian noble gases. In *Reviews in Mineralogy and Geochemistry*, Vol. 47, edited by Porcelli D., Ballentine C. J., and Wieler R. Washington (D.C.): Mineralogical Society of America. pp. 171-190.
- Terribilini D., Eugster O., Burger M., Jakob A., and Krähenbühl U. 1998. Noble gases and chemical composition of Shergotty mineral fractions, Chassigny, and Yamato 793605: The trapped argon - $^{40}\text{Ar}/\text{Ar}$ - ^{36}Ar ratio and ejection times of Martian meteorites. *Meteoritics & Planetary Science* 33(4):677-684.

- Trappitsch R., and Leya I. 2013. Cosmogenic production rates and recoil loss effects in micrometeorites and interplanetary dust particles. *Meteoritics & Planetary Science* 48:195-210.
- Trappitsch R. and Leya I. 2014. Depth-dependant solar cosmic ray induced cosmogenic production rates. *Lunar and Planetary Science Conference* 45, #1894.
- Wang D., and Chen M. 2006. Shock-induced melting, recrystallization, and exsolution in plagioclase from the Martian lherzolitic shergottite GRV 99027. *Meteoritics & Planetary Science* 41:519-527.
- Warren P. H. and Kallemeyn G. W. 1997. Yamato-793605, EET79001, and other presumed martian meteorites: Compositional clues to their origins. In *Antarctic Meteorite Research*, edited by Hirasawa T. Tokyo: National Institute of Polar Research. pp. 61-81.
- Wieler R. 2002. Cosmic-Ray-Produced Noble Gases in Meteorites. In *Reviews in Mineralogy and Geochemistry*, Vol. 47, edited by Porcelli D., Ballentine C. J., and Wieler R. Washington (D.C.): Mineralogical Society of America. pp. 125-170.
- Wieler R., Huber L., Busemann H., Seiler S., Leya I., Maden C., Masarik J., Meier M. M. M., Nagao K., Trappitsch R., and Irving A. J. 2016. Noble gases in 18 Martian meteorites and angrite Northwest Africa 7812—Exposure ages, trapped gases, and a re-evaluation of the evidence for solar cosmic ray-produced neon in shergottites and other achondrites. *Meteoritics & Planetary Science* 51:407-428.
- Zeitler P. K. 2015. U-Th/He Dating. In *Encyclopedia of Scientific Dating Methods*, edited by Rink W. J. and Thompson J. W. Dordrecht: Springer Netherlands. pp. 932-940.

Tables

Table 1. Typical noble gas blanks.

Isotope	Blank Concentration
³ He	1.65(4)×10 ⁻¹²
⁴ He	5(2)×10 ⁻¹⁰
²⁰ Ne	9.0(9)×10 ⁻¹²
²¹ Ne	3.5(5)×10 ⁻¹³
²² Ne	1.1(1)×10 ⁻¹²
³⁶ Ar	6(1)×10 ⁻¹²
⁴⁰ Ar	1.4(2)×10 ⁻⁹
⁸⁴ Kr	2.3(4)×10 ⁻¹³
¹³² Xe	1.2(5)×10 ⁻¹³

The abundances (in cm³ STP), are the average of stepwise heating blanks taken before and after a sample measurement. Blanks for each individual temperature step are used for the stepwise heating extractions. Uncertainties are 1σ, and the value in the parentheses reflects the uncertainty in the last digit.

Table 2. Concentrations of major and minor elements relevant to this work.

Element	GRV 99027 Bulk (a)	RSD%*	NWA 7034 Bulk (b)	Standard Deviation
O%	42.53		41.18	
Si%	20.2		22.23	0.85
Mg%	17.9	1	4.71	1.01
Fe%	14.9	1	10.11	1.92
Ca%	2.46	1	6.38	0.91
Al%	1.09	1	5.93	0.83
Na%	0.312	3	2.77	0.39
S	0	0	400	840
K	156	11	2800	500
Ti	2020	1	5900	1300
Mn	3530	6	2200	400
Ni	314	4	400	200
U	0.009	14	0.5124	0.024**
Th	0.031	5	2.635	0.063**
Sm	0.254	12	6.433	0.064**

Items marked with % are shown in weight percentage; all others are in μg/g, a. Lin et al. (2008); b. Agee et al. (2013); We use the composition of NWA 7034 (with adjustments for Na concentration, see text) for NWA 7906 and NWA 7907; * RSD% is the relative standard deviation of counting; **Errors for U and Th in NWA 7034 are reported as analytical absolute standard errors.

1

Table 3. Helium, Ne, and Ar isotopic concentrations for GRV 99027, NWA 7906, and NWA 7907.

Meteorite	Temp. (°C)	³ He	⁴ He	⁴ He/ ³ He	²¹ Ne	²⁰ Ne/ ²² Ne	²¹ Ne/ ²² Ne	(²² Ne/ ²¹ Ne) _c	³⁶ Ar	³⁶ Ar _t	³⁸ Ar _c	⁴⁰ Ar	⁴⁰ Ar
GRV 99027	800	1.2238(69)	5.80(10)	4.738(85)	0.03356(52)	0.720(29)	0.745(12)	1.350(22)	0.02841(69)			8.06(10)	
GRV 99027	1000	2.424(13)	10.576(94)	4.363(45)	0.1011(17)	0.817(15)	0.790(11)	1.264(18)	0.138(10)			42.91(46)	
GRV 99027	1200	2.971(52)	13.07(25)	4.40(11)	0.1874(34)	0.805(15)	0.767(13)	1.304(22)	0.0707(11)			23.41(25)	
GRV 99027	1400	0.3967(19)	1.531(50)	3.86(13)	0.5485(72)	0.8297(45)	0.7655(37)	1.3038(62)	0.1881(68)			84.32(89)	
GRV 99027	1600	n.m.	0.52(29)	n.m.	0.05876(92)	0.733(45)	0.794(11)	1.266(17)	0.024(14)			14.40(16)	
GRV 99027	1740	n.m.	0.12(15)	n.m.	0.00130(16)	n.m.	n.m.	n.m.	n.m.			0.916(24)	
Total		7.016(54)	31.62(44)	4.415(54)	0.9307(82)	0.813(13)	0.769(10)	1.299(17)	0.449(18)	~0.400*		174.0(11)	
NWA 7906	800	6.57(10)	2200(400)	340(70)	0.890(11)	1.059(28)	0.8029(46)	1.2235(70)	2.85(43)*			Overload	
NWA 7906	1000	0.1408 (10)	54(11)	387(80)	0.4287(54)	0.773(13)	0.8182(50)	1.2245(75)	0.21(10)			238.2(91)	
NWA 7906	1200	0.01535(25)	5.8(12)	378(80)	0.2696(33)	1.005(18)	0.8503(56)	1.1591(77)	0.797(56)			229.2(73)	
NWA 7906	1400	n.m.	n.m.	n.m.	0.05653(91)	1.30(15)	0.833(19)	1.159(30)	0.0440(43)			67.0(23)	
NWA 7906	1600	n.m.	n.m.	n.m.	0.00064(12)	8.0(36)	0.190(69)	n.m.	0.01016(34)			12.5(19)	
NWA 7906	1740	n.m.	n.m.	n.m.	0.000200(78)	13.3(64)	0.043(24)	0.95(53)	0.01752(51)			5.8(25)	
Total		6.73(10)	2300(400)	340(60)	1.646(13)	1.025(34)	0.8125(95)	1.212(14)	1.08(11)**	0.93(10)***	0.222(32)	550(12)	59
NWA 7907	800	5.67(12)	2600(530)	460(94)	0.839(10)	0.954(40)	0.810(11)	1.222(16)	0.129(26)			1600(100)	
NWA 7907	1000	0.13155(87)	60(10)	430(88)	0.4740(55)	0.816(15)	0.841(10)	1.188(15)	0.239(12)			191.4(85)	
NWA 7907	1200	0.01232(30)	3.3(10)	270(82)	0.2716(34)	0.829(17)	0.868(12)	1.149(16)	0.580(15)			184.6(66)	
NWA 7907	1400	n.m.	n.m.	n.m.	0.02008(35)	n.m.	0.94(6)	1.099(64)	0.01796(34)			31.8(21)	
NWA 7907	1600	n.m.	n.m.	n.m.	0.000462(41)	n.m.	n.m.	n.m.	n.m.			n.m.	
NWA 7907	1740	n.m.	n.m.	n.m.	n.m.	n.m.	n.m.	n.m.	n.m.			n.m.	
Total		5.82(12)	2700(530)	460(92)	1.604(12)	0.893(23)	0.8309(64)	1.1958(92)	0.965(32)	0.678(23)	0.441(44)	2000(100)	29

2

3

4

5

6

7

8

9

Abundances are in (10⁻⁸ cm³ STP/g). Uncertainties are 1σ and the value in the parentheses reflects the uncertainty in the last digit. Values marked “n.m.” were not measurable due either to (a) the reference isotope not exceeding the blank for the respective temperature step or (b) the uncertainty of the value exceeding the value itself, while those marked “no data” could not be measured due to technical problems with the mass spectrometer. “Overload” in the 800°C step for NWA 7906 marks where the sample had an unexpectedly high concentration of ⁴⁰Ar that overcharged the DVM; for all subsequent argon measurements, we retained a small aliquot for dilution where necessary, as it was for the 800°C step for NWA 7907. The volume of this aliquot is accounted for in the results. For concentrations, the “Total” value is the sum of all temperature steps for which there is data, while for ratios it is the ratio of summed concentrations for which there is data for both isotopes. The subscript “c” indicates the cosmogenic component, while the subscript “t” indicates the trapped component. * Approximate value based on average CRE age with SCR contribution. See the discussion on SCR production in the “Cosmic Ray Exposure Histories” section for details. ** ³⁶Ar

10
11

concentration is a lower limit; the correction for incompletely separated Ar in the Kr-Xe phase is done via ^{40}Ar , data for which is not available for this temperature step (see “overload” above). *** Does not include data from 800°C step due to lack of separation data for that step due to overload of ^{40}Ar .

Table 4. Krypton isotopic concentrations for GRV 99027, NWA 7906, and NWA 7907.

Meteorite	Temp. (°C)	⁸⁴ Kr	⁸⁴ Kr/ ¹³² Xe	⁸⁰ Kr/ ⁸⁴ Kr	⁸² Kr/ ⁸⁴ Kr	⁸³ Kr/ ⁸⁴ Kr	⁸⁶ Kr/ ⁸⁴ Kr
GRV 99027	800	0.00344(13)	2.05(10)	No data	0.209(10)	No data	0.315(15)
GRV 99027	1000	0.00187(30)	2.68(44)	No data	No data	No data	No data
GRV 99027	1200	0.00238(26)	1.65(18)	No data	0.154(18)	No data	No data
GRV 99027	1400	0.00528(31)	1.86(15)	No data	No data	No data	No data
GRV 99027	1600	0.000101(87)	n.m.	No data	0.26(23)	No data	No data
GRV 99027	1740	n.m.	n.m.	n.m.	n.m.	n.m.	n.m.
Total		0.01296(53)	1.947(93)	No data	0.188(17)	No data	0.315(15)
NWA 7906	800	0.0281(22)	1.44(15)	0.0455(46)	0.203(23)	0.230(22)	0.293(32)
NWA 7906	1000	0.0089(13)	1.94(43)	0.070(13)	0.226(45)	0.210(44)	0.268(61)
NWA 7906	1200	0.0108(27)	2.7(13)	0.112(31)	0.247(81)	0.237(81)	0.28(11)
NWA 7906	1400	0.0049(30)	1.3(11)	n.m.	n.m.	0.21(18)	0.29(26)
NWA 7906	1600	n.m.	n.m.	n.m.	n.m.	n.m.	n.m.
NWA 7906	1740	n.m.	n.m.	n.m.	n.m.	n.m.	n.m.
Total		0.0526(48)	1.66(22)	0.065(12)	0.217(35)	0.211(39)	0.268(53)
NWA 7907	800	0.02022(36)	1.42(12)	0.0540(16)	0.2176(68)	0.2206(67)	0.3077(86)
NWA 7907	1000	0.00796(11)	2.39(50)	0.0821(24)	0.2248(64)	0.2270(63)	0.2872(76)
NWA 7907	1200	0.00683(11)	3.6(32)	0.1578(46)	0.2874(81)	0.2659(72)	0.2886(87)
NWA 7907	1400	0.001087(34)		0.1245(79)	0.379(25)	0.284(18)	0.281(23)
NWA 7907	1600	n.m.		n.m.	n.m.	n.m.	n.m.
NWA 7907	1740	n.m.		n.m.	n.m.	n.m.	n.m.
Total		0.03609(39)	1.80(20)	0.0819(18)	0.2373(57)	0.2325(55)	0.2988(71)

Abundances are in (10⁻⁸ cm³ STP/g). Uncertainties are 1σ and the value in the parentheses reflects the uncertainty in the last digit. Values marked “n.m.” were not measurable due either to (a) the reference isotope not exceeding the blank for the respective temperature step or (b) the uncertainty of the value exceeding the value itself, while those marked “no data” could not be measured due to technical problems with the mass spectrometer. For concentrations, the “Total” value is the sum of all temperature steps for which there is data, while for ratios it is the ratio of summed concentrations for which there is data for both isotopes. ⁷⁸Kr/⁸⁴Kr cannot be given due to uncorrected interferences on mass 78.

12
13
14
15
16
17
18
19
20
21
22

Table 5. Xenon isotopic concentrations for GRV 99027, NWA 7906, and NWA 7907.

Meteorite	Temp. (°C)	¹³² Xe	¹²⁴ Xe/ ¹³² Xe	¹²⁶ Xe/ ¹³² Xe	¹²⁸ Xe/ ¹³² Xe	¹²⁹ Xe/ ¹³² Xe	¹³⁰ Xe/ ¹³² Xe	¹³¹ Xe/ ¹³² Xe	¹³⁴ Xe/ ¹³² Xe	¹³⁶ Xe/ ¹³² Xe
GRV 99027	800	0.00167(6)	0.00309(60)	0.0033(11)	0.0613(42)	1.100(47)	0.160(11)	0.853(38)	0.409(20)	0.359(15)
GRV 99027	1000	0.000697(27)	No data	0.397(50)	0.342(36)					
GRV 99027	1200	0.001443(24)	0.00029(64)	n.m.	0.0265(31)	No data	0.131(11)	No data	No data	No data
GRV 99027	1400	0.00284(16)	0.00361(72)	0.00078(64)	0.0726(45)	No data	0.147(12)	No data	No data	No data
GRV 99027	1600	n.m.	n.m.	n.m.	n.m.	n.m.	n.m.	n.m.	n.m.	n.m.
GRV 99027	1740	n.m.	n.m.	n.m.	n.m.	n.m.	n.m.	n.m.	n.m.	n.m.
Total		0.00666(17)	0.00266(43)	0.00131(44)	0.0583(37)	1.100(47)	0.147(9)	0.853(55)	0.405(25)	0.354(20)
Meteorite	Temp. (°C)	¹³² Xe	¹²⁴ Xe/ ¹³² Xe	¹²⁶ Xe/ ¹³² Xe	¹²⁸ Xe/ ¹³² Xe	¹²⁹ Xe/ ¹³² Xe	¹³⁰ Xe/ ¹³² Xe	¹³¹ Xe/ ¹³² Xe	¹³⁴ Xe/ ¹³² Xe	¹³⁶ Xe/ ¹³² Xe
NWA 7906	800	0.0194(12)	0.00466(49)	0.00430(47)	0.0800(68)	1.029(85)	0.155(12)	0.812(69)	0.380(31)	0.307(25)
NWA 7906	1000	0.00457(73)	0.00538(90)	0.0073(14)	0.082(19)	1.07(22)	0.148(33)	0.74(17)	0.383(82)	0.270(62)
NWA 7906	1200	0.0040(17)	0.0176(76)	0.0200(85)	0.099(54)	1.30(69)	0.17(10)	0.84(49)	0.38(23)	0.30(17)
NWA 7906	1400	0.0037(20)	0.0070(46)	0.0086(51)	0.069(57)	0.90(75)	0.18(14)	0.58(54)	0.41(32)	0.28(23)
NWA 7906	1600	n.m.	n.m.	n.m.	n.m.	n.m.	n.m.	n.m.	n.m.	n.m.
NWA 7906	1740	n.m.	n.m.	n.m.	n.m.	n.m.	n.m.	n.m.	n.m.	n.m.
Total		0.0317(30)	0.0067(17)	0.0072(19)	0.081(15)	1.05(20)	0.159(31)	0.78(14)	0.384(73)	0.297(56)
NWA 7907	800	0.0142(12)	0.00397(44)	0.00462(51)	0.0789(88)	1.12(11)	0.146(15)	0.745(89)	0.374(39)	0.308(33)
NWA 7907	1000	0.00333(70)	0.0080(17)	0.0091(21)	0.098(28)	1.31(34)	0.144(43)	0.73(22)	0.40(11)	0.263(81)
NWA 7907	1200	0.0019(16)	0.036(32)	0.047(41)	n.m.	n.m.	n.m.	n.m.	n.m.	n.m.
NWA 7907	1400	n.m.	n.m.	n.m.	n.m.	n.m.	n.m.	n.m.	n.m.	n.m.
NWA 7907	1600	n.m.	n.m.	n.m.	n.m.	n.m.	n.m.	n.m.	n.m.	n.m.
NWA 7907	1740	n.m.	n.m.	n.m.	n.m.	n.m.	n.m.	n.m.	n.m.	n.m.
Total		0.0200(29)	0.0078(45)	0.0095(57)	0.096(23)	1.16(17)	0.145(22)	0.74(12)	0.380(56)	0.299(45)

Abundances are in (10⁻⁸ cm³ STP/g). Uncertainties are 1σ and the value in the parentheses reflects the uncertainty in the last digit. Values marked “n.m.” were not measurable due either to (a) the reference isotope not exceeding the blank for the respective temperature step or (b) the uncertainty of the value exceeding the value itself, while those marked “no data” could not be measured due to technical problems with the mass spectrometer. For concentrations, the “Total” value is the sum of all temperature steps for which there is data, while for ratios it is the ratio of summed concentrations for which there is data for both isotopes.

23
24
25
26
27

Table 6. Production rates and CRE exposure ages (Ma).

Meteorite	Ref	GCR							SCR					³ He Age	²¹ Ne Age	³⁸ Ar Age	
		P _{3-GCR}	P _{21-GCR}	P _{36-GCR}	P _{38-GCR}	³ He	²¹ Ne	³⁸ Ar	(²² Ne/ ²¹ Ne) _c	P _{3-SCR}	P _{21-SCR}	P _{22-SCR}	P _{36/21}				P _{38/21}
ALHA 77005	a	1.57	0.180		0.0629	7.49(30)	0.988(50)	0.166(15)	1.287(40)						4.77(35)	5.49(40)	2.64(40)
ALHA 77005	e	1.280	0.154		0.030										5.79(58)	6.33(63)	5.58(56)
LEW 88516	b	1.60	0.204		0.079	7.23(12)	1.00(4)	0.31(1)	1.227(35)						4.52*	4.90*	3.92*
LEW 88516	f	1.379	0.189		0.041										5.24(52)	5.30(53)	7.54(75)
Y-793605	c	1.61	0.274		0.0729	7.60(30)	1.09(10)	0.228(15)	1.207(20)						4.72(25)	3.98(25)	3.13(20)
Y-793605	e	1.398	0.194		0.042										5.44(54)	5.61(56)	5.48(55)
NWA 1950	d	1.588	0.194		0.0716	6.53(30)	1.02(10)	0.205(25)	1.249(20)						4.1(3)	5.3(4)	2.9(2)
NWA 1950	e	1.340	0.172		0.034										4.87(49)	5.94(59)	5.97(59)
NWA 4797	g	1.41	0.205		0.0490	6.61	1.184	0.423	1.18						4.7(5)***	5.8(6)***	8.6(9)***
NWA 6342	g	1.41	0.205		0.0410	7.28	1.127	0.188	1.26						5.2(5)***	5.5(6)***	4.6(5)**
GRV 99027	e, f	1.283	0.157	0.00950	0.0297	7.016(54)	0.9307(82)	n.m.	1.299(17)	0.643	1.637	2.287	0.241	0.257	5.47(55)	5.94 (59)	No data
NWA 7906	e	1.584	0.249		0.158	6.73(10)	1.646(13)	0.222(32)	1.212(14)						4.25(42)	6.60(66)	1.40(14)
NWA 7907	e	1.588	0.261		0.169	5.82(12)	1.604(12)	0.441(44)	1.1958(92)						3.67(37)	6.08(63)	2.60(26)

29 GCR and SCR production rates for ³He, ²¹Ne, ³⁶Ar and ³⁸Ar (P₃, P₂₁, P₃₆, P₃₈) are in 10⁻⁸ cm³ STP g⁻¹ Ma⁻¹; exposure ages are in Ma. Uncertainties are 1σ and the value in the parentheses
30 reflects the uncertainty in the last digit. The uncertainties of values from the literature are those given in the original publication. Some references report 2σ uncertainties; these have been
31 converted to 1σ uncertainties for ease of comparison. SCR production rates assume J₀ = 100 cm⁻² s⁻¹, R₀ = 125 MV, a solar distance of 1 AU, and negligible shielding. CRE ages and
32 production rates as reported by a) Eugster et al. (2002); b) Eugster et al. (1997); c) Terribilini et al. (1998); d) Christen et al. (2005); e) this work, either recalculated using data from literature
33 or original calculations for GRV 99027, NWA 7906, and NWA 7907; f) Assuming a pre-atmospheric radius <3 cm, using the volume weighted production rate model, corrected for SCR-
34 produced cosmogenic gas; g) Wieler et al. (2016). CRE ages and production rates reported in the literature use the production rate model of Eugster and Michel (1995). Those calculated in
35 this work use that of Leya and Masarik (2009) and updates using the cosmogenic (²²Ne/²¹Ne)_c ratio reported in the literature (for recalculations of literature values) or determined by us (for
36 GRV 99027, NWA 7906, and NWA 7907) as a shielding indicator and are assumed to have uncertainties of 10%. Unless otherwise indicated, the uncertainty of the average age is determined
37 by propagating the uncertainty of the isotope-specific ages from which the average is calculated. * No uncertainty reported in original source. Uncertainty for the average is the 1σ standard
38 error of the mean. ** 1σ standard error of the mean. *** No uncertainty reported in original source. Since Wieler et al. (2016) used the Leya and Masarik (2009) production rate model to
39 calculate ages, we assume a 10% uncertainty in their calculated ages. † ³⁸Ar excluded from average age calculation. ‡ ³⁸Ar excluded from average age calculation by Wieler et al. (2016) due
40 to likely target inhomogeneity.

41

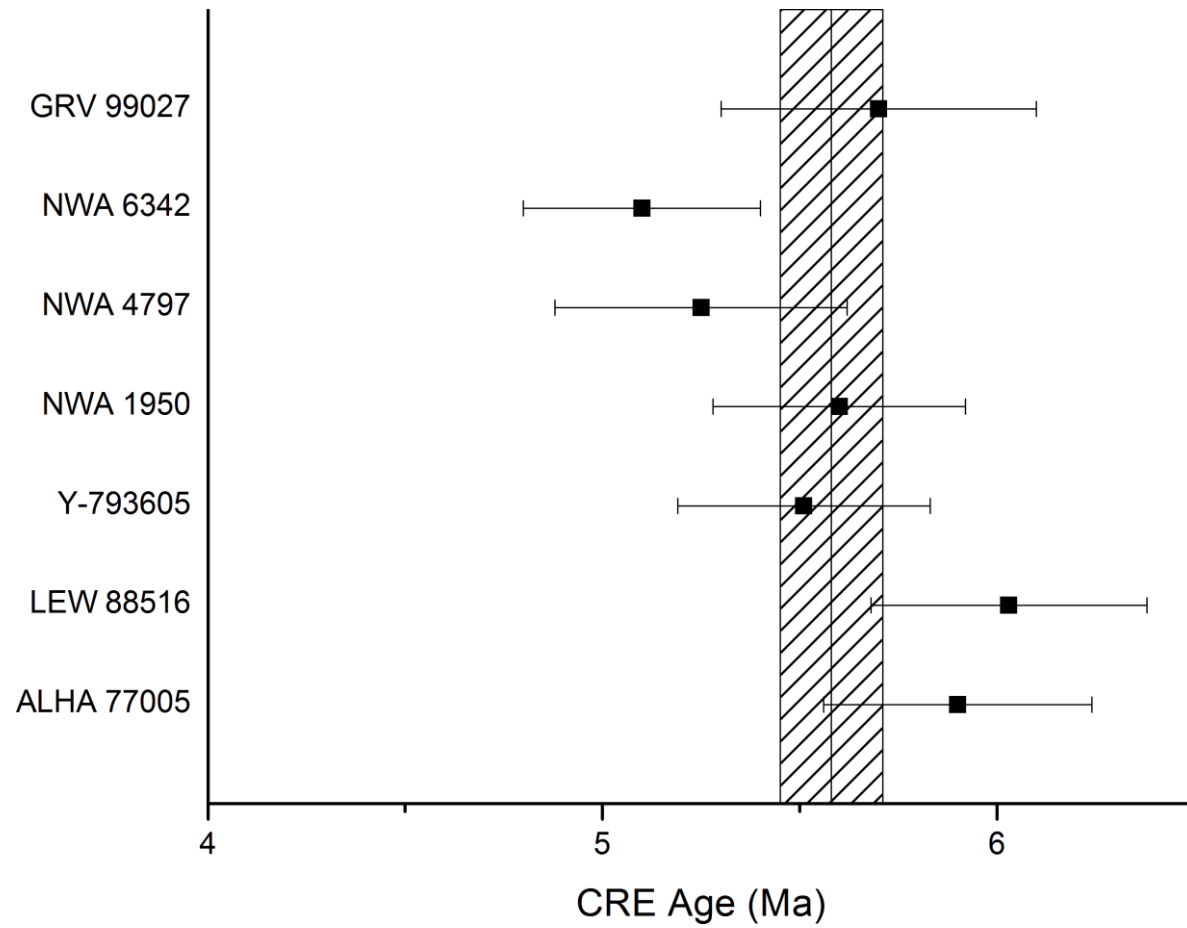
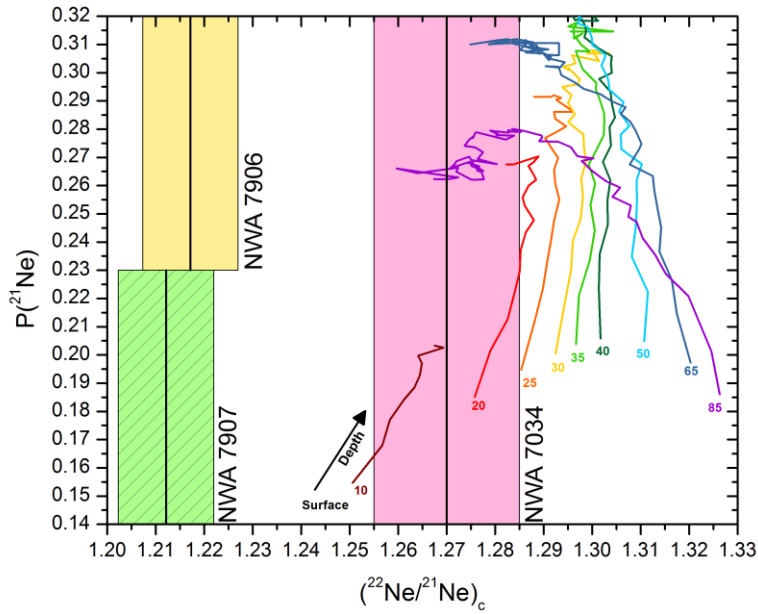
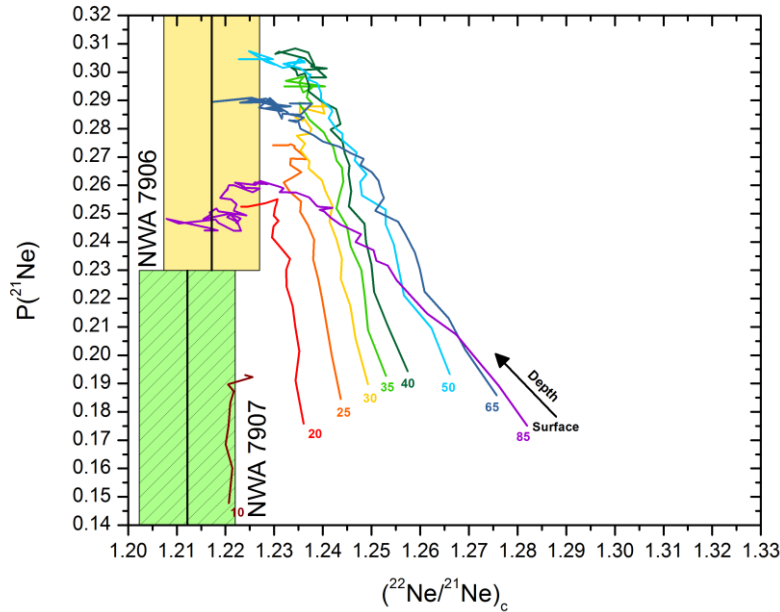


Figure 1. CRE age histogram for poikilitic basaltic shergottites (including the new data for GRV 99027). All uncertainties are 1σ . The solid line and shaded area represent the average CRE age of the poikilitic basaltic shergottites calculated in this work and its 1σ uncertainty, respectively.



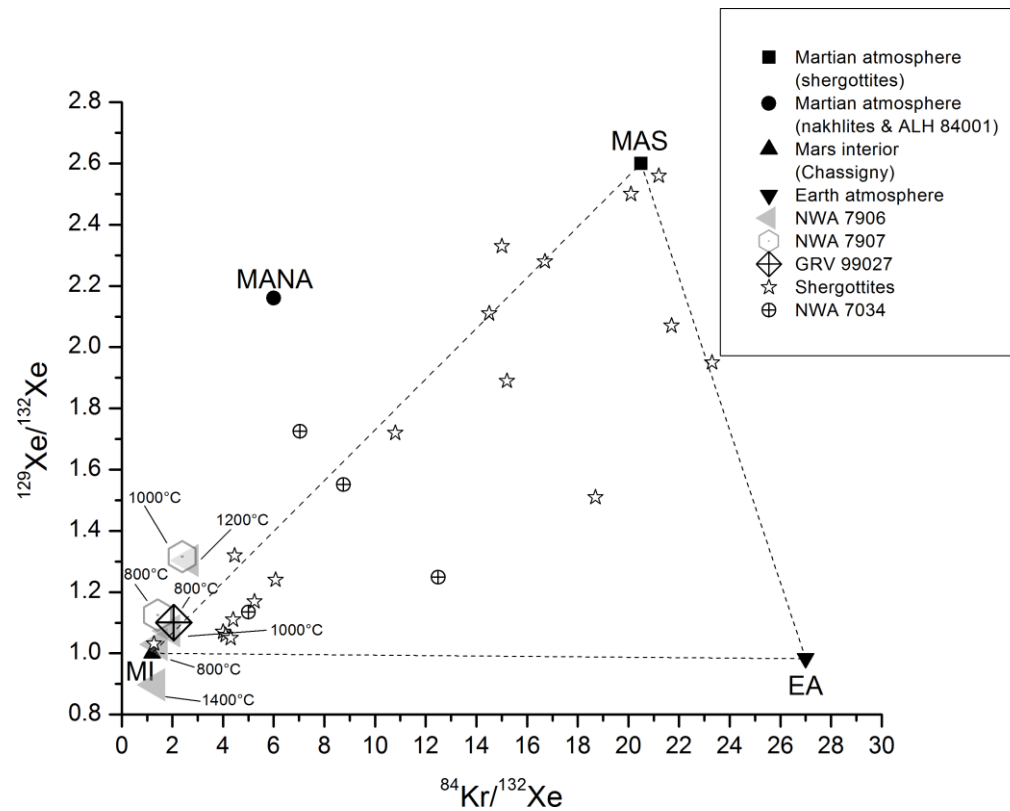
48



49

50 Figure 2. Modelled production rates for cosmogenic $^{21}\text{Ne}_c$, $P(^{21}\text{Ne})$, as a function of $(^{22}\text{Ne}/^{21}\text{Ne})_c$.
 51 Numbers shown at the lower end of each modeled line represent the meteoroid radius in centimeters,
 52 with the bottom of each line representing the surface of the meteoroid. Upper panel: Production rates
 53 calculated by Cartwright et al. (2014) in their Fig. S3 based on the chemical composition measured by
 54 Agee et al. (2013) for NWA 7034. The $(^{22}\text{Ne}/^{21}\text{Ne})_c$ ratio reported by Cartwright et al. (2014) is 1.27,
 55 with the pink band representing the reported uncertainty. The $(^{22}\text{Ne}/^{21}\text{Ne})_c$ ratio for NWA 7906 (yellow
 56 band) and NWA 7907 (green band) are both lower than the model predictions calculated using the Leya
 57 and Masarik (2009) model using ordinary chondrite systematics. Lower panel: The same plot but
 58 assuming a Na concentration of 1.5wt% for NWA 7906 and NWA 7907. After this adjustment, the
 59 measured ratios fall in the range predicted by the model calculations.

60



62

63

64

65

66

67

Figure 3. Three-isotope plot of $^{129}\text{Xe}/^{132}\text{Xe}$ vs. $^{84}\text{Kr}/^{132}\text{Xe}$ for GRV 99027, NWA 7906, and NWA 7907. For comparison, literature data for other shergottites (Bogard and Garrison 1998; Llorca et al. 2013; Mathew et al. 2003) and NWA 7034 (Cartwright et al. 2014) are also plotted. Additionally, data for the Earth's atmosphere (EA, Pepin et al. 1995, Swindle 2002), Martian atmosphere via shergottites (MAS, Bogard and Garrison 1998), and Martian atmosphere via nakhrites and ALH 84001 (MANA, Mathew and Marti 2001), and Martian interior (Chassigny) (MI, Ott 1988) are plotted.

68